# AN X-RAY SHADOWGRAPH TO LOCATE TRANSIENT HIGH-ENERGY CELESTIAL SOURCES

G. J. Fishman and T. A. Parnell
Space Sciences Laboratory
NASA/Marshall Space Flight Center
Huntsville, Alabama

T. A. Rygg* and J. C. Gregory
University of Alabama
Huntsville, Alabama

A new technique has been developed to locate strong, transient x-ray sources such as the recently discovered gamma-ray bursts. The instrument, termed a "shadowgraph," locates sources by detecting the x-ray shadow cast by a large occulting mask pattern on an imaging detector. Angular resolutions of from 2 to 10 arc minutes are obtainable while essentially full sky coverage is maintained. The optimum energy range of operation is between 20 keV and 100 keV.

The high-efficiency x-ray imaging detectors, which make it possible to locate bursts with intensities down to ~10 photons/cm$^2$-sec, are capable of detecting single 20-keV photons with a spatial resolution of ~0.2 mm. The detectors consist of an x-ray to optical conversion phosphor, a multistage image intensifier, and a CCD image readout.

## I. INTRODUCTION

The relatively new field of x-ray astronomy has led to the discovery of entirely new classes of celestial objects and has provided us with new insights into the final evolutionary stages of stars and the origin of high-energy processes in the galaxy.

*Dr. Rygg died on March 14, 1975.

Among the more interesting phenomena are the recently discovered gamma-ray bursts (Ref. 1). These infrequent, transient events produce intense fluxes of x-rays and gamma-rays relative to the background. Position data is poor, although the sources appear to have an isotropic distribution. Although many theories for the bursts have been proposed (Ref. 2), it appears that a satisfactory explanation may have to await accurate measurement of their positions so that they may be identified with a particular type of optical or radio object. Such a measurement presents a unique experimental problem. Because of their apparently random occurrence in space and their brief duration — as short as 0.1 sec — it is necessary to use a wide-field detector. Since observable bursts occur infrequently and apparently randomly in time, the detector must be in continuous operation above the atmosphere for long periods.

The instrument we have developed for locating discrete, brief bursts of x-rays and gamma-rays is termed a "shadowgraph" and combines the features of wide field, high efficiency, and good angular resolution. Image readout by a CCD confers an advantageous combination of simplicity, integrating capability, and energy discrimination of the x-ray spatial detector compared with other position-sensitive x-ray detectors. The x-ray system has thus far been tested only by photographic means rather than by CCD readout. Since CCD technology is expected to improve greatly before the first operational shadowgraph, this paper will stress the experimental techniques and capabilities of the shadowgraph and the specifications of CCDs optimized for this application.

## II. PRINCIPLE OF OPERATION

The shadowgraph is composed of a large dome-like occulting shadow mask and a number of x-ray imaging detectors located inside to detect an x-ray shadow cast through any part of the shadow mask (see Figure 1). A typical mask is made from photoetched 0.5-mm-thick tungsten plate. This thickness would provide adequate opacity for x-rays with energies up to 150 keV. The solid angle subtended by the mask at the detectors determines the field of view of the instrument, which could, conceivably, cover $4\pi$ steradians.

Since it is assumed that the brief bursts arrive from a point source at a great distance (Ref. 1), the parallel incident x-ray beam would produce a sharp shadow of the coded mask on the face of an x-ray image detector. The x-ray

shadow projection angle is uniquely determined simply by finding the area on the mask which produced the shadow. The source direction is then derived from this shadow projection angle and the orientation of the spacecraft.

The angular resolution of the shadowgraph is $\Delta\theta \approx \Delta x/d$, where $\Delta x$ is the spatial uncertainty of the image position and d is the distance between the image plane and the appropriate shadow mask section. There are several components which enter into $\Delta x$; among the most important are: (1) x-ray source photon statistics and background events, (2) flexing and thermal distortion of the shadow mask and image detector image system, and (3) uncertainty in the location of individual x-ray photon events. It is estimated that for a weak burst, with ~400 x-ray photons over a 100-$cm^2$ detector area, the value for $\Delta x$ will be of the order ~1 mm. For a small Explorer-type satellite, an average value for d is ~70 cm, yielding a location uncertainty of $\Delta\theta \approx 1$ mm/70 cm = 5 arc minutes. Spacecraft motion during observation, and attitude uncertainty will increase the location error somewhat.

The uncertainty due to photon statistics and background events, $\Delta x_1$, has been examined in detail, both analytically and through computer simulations. Consider $N_s$ photons incident on a shadow mask with a transmission factor r (ratio of open area to total area) and a characteristic pattern cell dimension $\ell$. Also assume that there are $N_b$ background events randomly spaced over the image detector area and that it is required to locate the pattern with a statistical uncertainty of $n_\sigma$ standard deviations. Then

$$\Delta x_1 \approx \frac{n_\sigma^2 \ell (N_s + N_b)}{r N_s^2} \qquad (1)$$

Figure 2 shows the results of a simulation of x-ray images from various fluxes of signal photons from a point source incident on the shadow mask pattern, with r = 0.44. A portion of the pattern is shown at the top of the figure. The amount of random background or noise photons was also varied, being equal to 1/2, 1/5, or 1/10 of the number of signal photons, as indicated in the figure. A computer program was used to find the optimum fit between the total mask pattern and the discrete photon image pattern by shifting the image in small steps over the larger mask pattern and finding the minimum photon coverage.

Assuming that the image area is 10 cm × 10 cm, the optimized fit from the computer routine for the case of 200 signal photons and 100 noise photons was less than 0.6 mm, while the value obtained from Equation (1) is ~0.5 mm for a 2 $\sigma$ error. Note that at this low signal level, the mask pattern is not visually recognizable. This demonstrates that relatively little information is required to ascertain the location of the source by this technique, since the image detected is a portion of a known pattern. Naturally, it would be impossible to reconstruct a meaningful image from only 200 photon locations.

Since the locating accuracy for weak x-ray or gamma-ray bursts is dependent mainly upon photon statistics, it is desirable to obtain the highest ratio of signal photons to background photons in a particular energy range. Among the considerations that determine the optimum energy range are: (1) the spectrum expected from the source object, (2) the spectra of various components of the background such as the diffuse x-ray background and secondary x-ray and gamma-ray fluxes produced by charged-particle interactions; and (3) the efficiency of the shadowgraph mask and image detector combination. A rather detailed analysis of the combined spectral effects yields an optimum x-ray energy range of ~20 keV to ~100 keV in which to make observations of gamma-ray bursts.

## III. IMAGING DETECTORS

The imaging detector is the most critical component for the shadowgraph and other x-ray multiplex methods such as the scatter-hole or Dicke camera (Refs. 3, 4). For this application, the essential characteristics are: (1) good spatial resolution irrespective of angle of incidence of the x-ray photon, (2) high detection efficiency over the energy range of interest, (3) large sensitive area, and (4) capability for observing a large range of burst intensities.

After studying several alternatives, the phosphor-image intensifier system (Figure 3) was chosen as the most suitable wide-field image detector for the energy region up to 100 keV. In this system, the x-ray photon is first converted into optical photons in a relatively thick (0.5 to 1.0 mm) phosphor. Present phosphors under study include rare-earth phosphors and cesium iodide. The energy conversion efficiency of these phosphors is in the range from 5% to 15%, so that a 20-keV photon will result in ~$10^3$ photons in the range 4000 Å to 5000 Å. The optical signal having a spot size of ~1 $mm^2$ is intensified and

demagnified by a multistage, electrostatically focused image intensifier. The image is then transferred by a lens onto a CCD for image readout.

Overall image reduction is from 80 mm X 80 mm at the x-ray phosphor to about 6 mm X 6 mm at the CCD. Linear spatial resolution at the x-ray phosphor of 0.5 mm thus requires a 160 X 160 element CCD array of area about 6 mm square. Grey level encoding of 4 bits would be sufficient to provide coarse energy resolution for each detected x-ray. The energy information would be used in the data analysis to eliminate sources of background such as dark current, high-energy gamma-ray Compton events, and charged particles. It is anticipated that the x-ray image integration time will be of the order of 1 sec, which may require operating the CCDs at temperatures below 0° C. Such temperatures would also reduce the dark current of the image intensifiers. The total image data expected from a single x-ray burst is several megabits. Present CCD technology requires that this data be stored in a nonvolatile, onboard digital storage device (possibly a CCD memory) for later transmission to a ground station.

The pictures in Figure 4 are output images of an experimental setup in our laboratory to study properties of intensifiers and x-ray converter phosphors. Two three-stage image intensifiers (Varo models 8585 and 8605) were coupled by an f/1.4 lens. A 0.5-mm-thick rare-earth phosphor was placed directly on the fiber optic input of the first intensifier (25-mm diameter), and the output of the second intensifier was photographed on Tri-X film with a 35-mm single-lens reflex camera. Figure 4 shows three photographs obtained with this system: two with weak radioactive sources present and one with background only. Individual x-ray photons can easily be observed from $Co^{57}$ (122 keV) and $Am^{241}$ (60 keV). All three photographs were obtained under the same conditions, outlined in Figure 4. The centroid of the brighter x-ray images can be determined to within ~0.2 mm.

It appears that the imaging requirements for an x-ray shadowgraph in terms of array size, resolution, and dynamic range can be met by current CCD technology. For a space-borne experiment, a CCD image readout offers great advantages of simplicity, small size, low power, low weight, and image positional stability compared to any conventional TV tubes. Areas of potential concern include long-term gain stability, image degradation during integration, and reliability.

## REFERENCES


1. Klebesadel, R. W.; Strong, I. B.; and Olson, R. A.: Astrophys. J., Vol. 182, p. L85 (1973).

2. Ruderman, M. A.: Proceedings Seventh Texas Symposium on Relativistic Astrophysics, New York Academy of Sciences (to be published, 1975).

3. Dicke, R. H.: Astrophys. J., Vol. 153, p. L101 (1968).

4. Ables, I. G.: Proc. Astron. Soc. Australia, #4, p. 1 (1968).

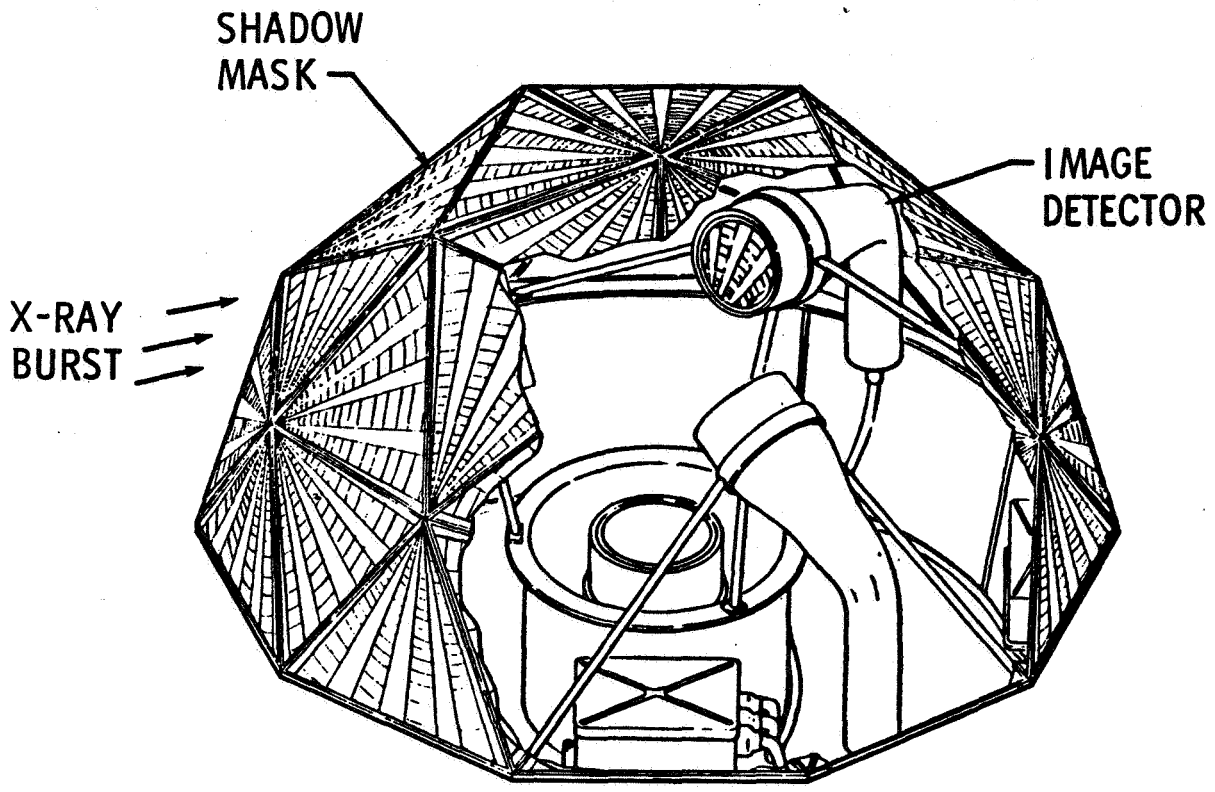


Figure 1. Shadowgraph experiment components (As shown, an x-ray burst incident from the left would cast an x-ray shadow on the forward-facing image detector. )

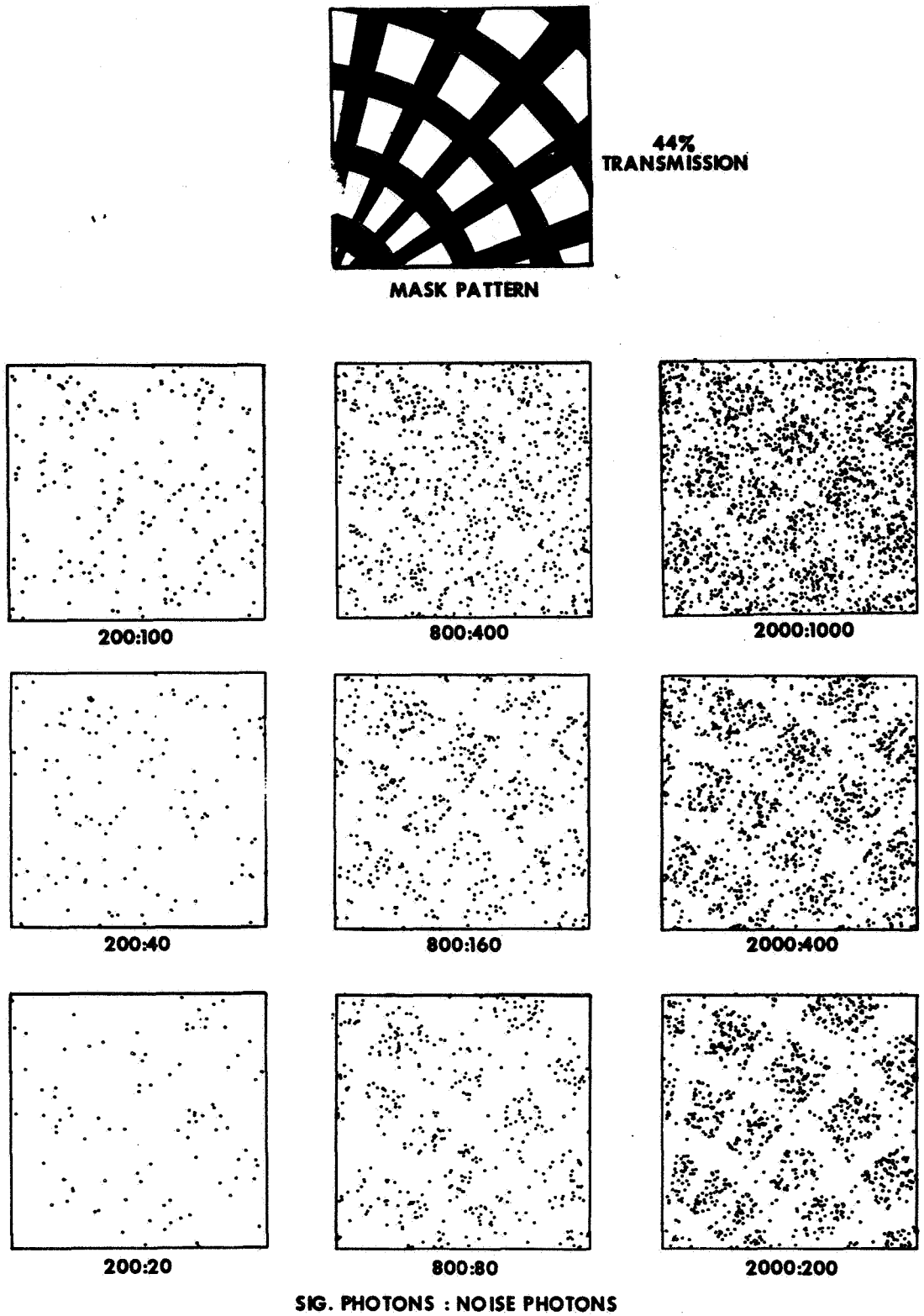


Figure 2. Simulated shadowgraph images showing effects of signal and noise photon statistics (The incident source photons are transmitted through the open areas of the mask pattern at the top, which represents a portion of the large shadow mask.)

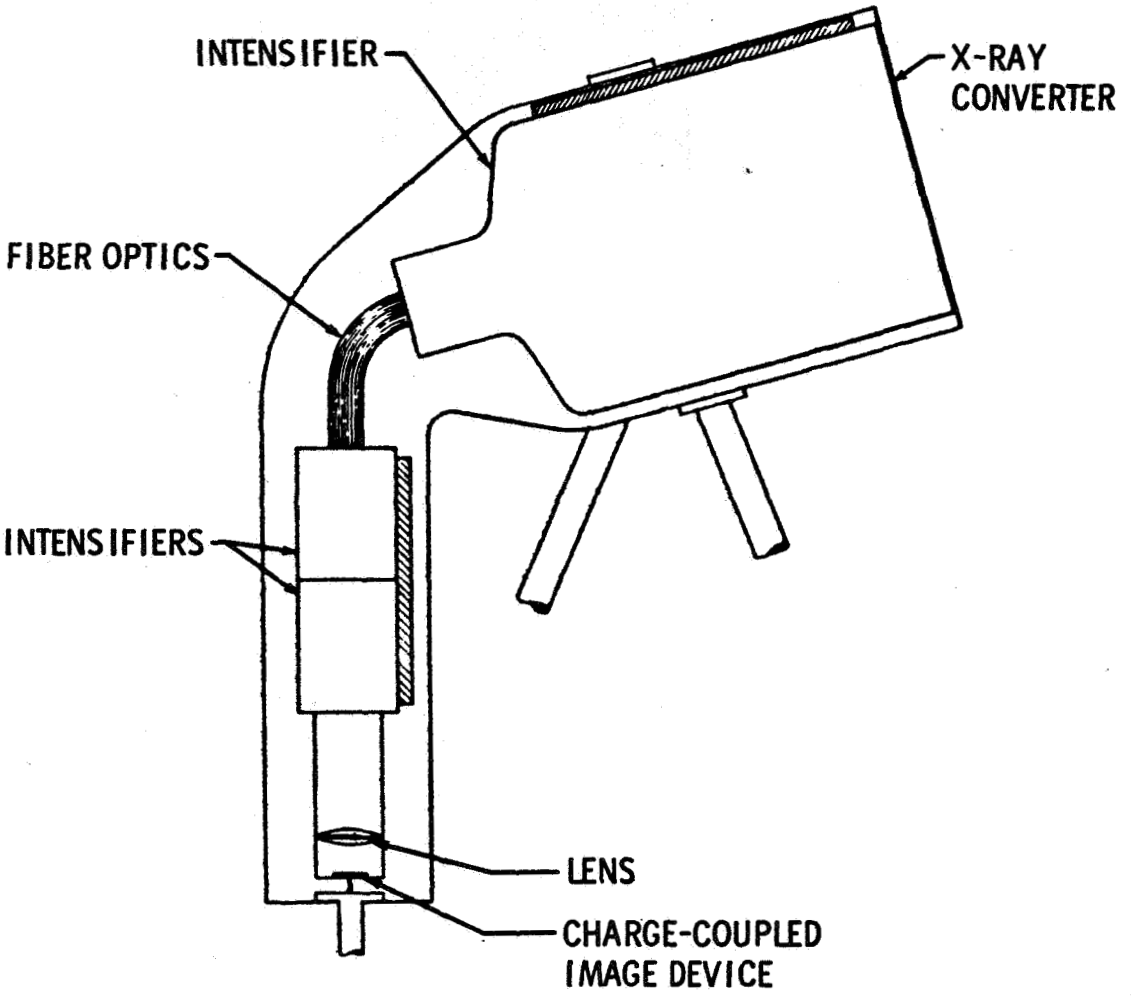


Figure 3. X-ray image detector schematic (The first-stage intensifier is an 80-mm/20-mm zoom-type intensifier. Additional stages are required to produce a suitable intensity for the CCD. It may be possible to improve the overall efficiency by coupling the CCD with fiber optics or even by locating the CCD internally in the last intensifier stage.)

# X-RAY TEST PICTURES

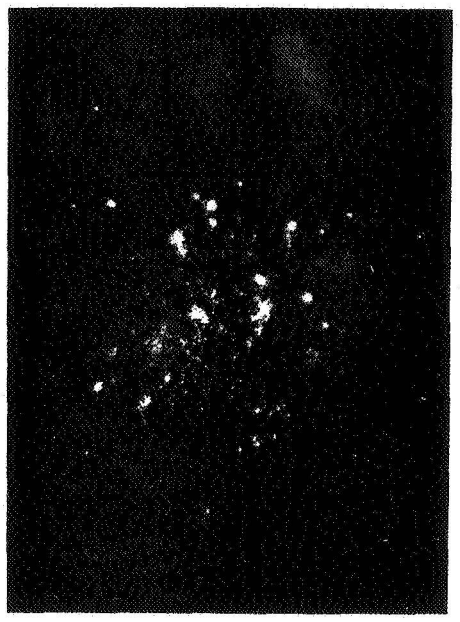

EXPOSURE: 0.125 sec
PHOSPHOR: RARE EARTH
THICKNESS: 0.5 mm
TEMP.: $20^0$ C
GAIN: $\sim 10^6$
SCALE: ⊢ 1 mm

$Am^{241}$ 60 KeV

$Co^{57}$ 122 KeV

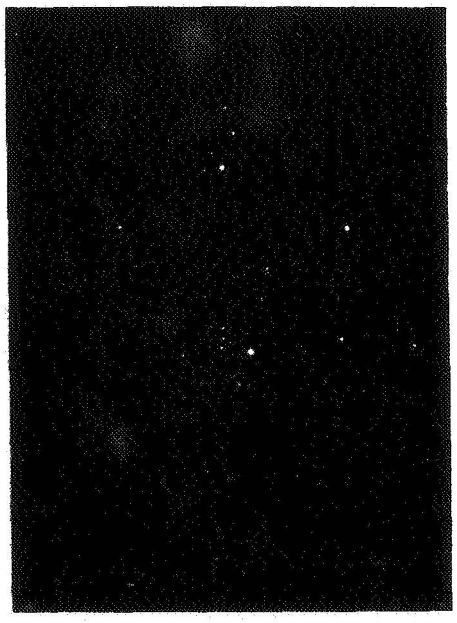

BACKGROUND

Figure 4. X-ray test photographs of a rare-earth phosphor/multi-stage intensifier system (Single x-ray photons at 60 keV and 122 keV are visible. Intensifier input diameter is 25 mm. X-ray spot size is ~0.5 mm. The centroid of each spot can be determined to less than 0.2 mm.)